

Short Papers

Microwave Noise Characterization of Two-Port Devices Using an Uncalibrated Tuner

R. Benelbar, B. Huyart, and R. G. Bosisio

Abstract—A novel noise-parameter and *S*-parameter measurement system is proposed. Any device under test (DUT) can be characterized using the proposed setup. Such characterization is performed without any preset conditions on the input impedance of the noise-receiver and the repeatability of the impedance tuning mechanism. The DUT is used as a standard for tuner calibration. Measurements were carried out on a general purpose GaAs-MESFET. The extracted transistor noise-parameters are in good agreement with the manufacturer's specified values over the operating frequency band (4–8 GHz).

I. INTRODUCTION

The usual four noise-parameters are normally determined from the measurement of the noise-figure for one or more source reflection coefficients of the device under test (DUT). Several techniques have been developed over the last two decades. One of these methods is only used for the noise characterization of metal semiconductor field-effect transistors (MESFET's) and high electron mobility transistors (HEMT's). The noise behavior of these devices can be predicted from their small-signal equivalent circuit model and the noise sources of the drain and gate resistances. In this case, only one noise-figure measurement is required when the noise temperature of the gate resistance is equal to the ambient temperature [1], [2].

In a second technique, a tuner, inserted between the DUT and the noise source, is used to vary the DUT source reflection coefficient. This setup allows the measurement of the tuner impedance and insertion loss using three switches. This is possible only when the noise-receiver input is matched and the switches are lossless [3].

A third method uses a one-port tuner which has to be calibrated. This is due to the fact that such method requires a set of predetermined tuner positions for DUT noise-figure measurement [4].

The DUT noise-figure measurements for many source impedances (four at least), is a well-suited strategy for computer-controlled measurements [5]. Such an automated procedure is widely used in microwave noise-parameter characterization. This strategy is used in this work to perform measurements as illustrated in Fig. 1. The important elements of this bench are: the noise source (KTB), the uncalibrated mechanical tuner, the tee-bias, the transistor (DUT) mounted on a fixture, and the noise-receiver.

II. NEW MEASUREMENT SETUP

The noise-receiver measures the noise-figure of the entire system (Fig. 1). Thus, we must find a method which allows us to extract the

Manuscript received June 11, 1995; revised June 14, 1996.

R. Benelbar is with the MPB Technologies Inc. Communication Division, 1725 North Service Road Trans Canada Highway, Dorval PQ, H9P 1J1 Canada.

B. Huyart is with the Laboratoire d'hyperfréquences, Department of Communication, École Nationale Supérieure des Télécommunications, 75634 Paris Cedex 13, France.

R. G. Bosisio is with the Microwave Research Laboratory, Electrical & Computer Engineering Department, Ecole Polytechnique de Montréal, Montreal PQ, H3V 1A2 Canada.

Publisher Item Identifier S 0018-9480(96)06909-8.

transistor's noise contribution (F_2) from the total noise (F_t). One can notice that the first and the third stages in Fig. 1 are passive and, consequently, the corresponding noise-figures can be obtained by measuring their respective available power gains. This task can be done by *S*-parameter measurement of each stage, including their source impedances, using a commercial network analyzer (ANA). The noise and *S*-parameter measurements are then performed separately using two switches (Fig. 1).

A. The Proposed Solution

We suggest to calculate the available power gain of the first stage using the active DUT as a variable microwave load. By choosing a specific bias point, the device's *S*-parameters and its input reflection coefficient can be easily controlled. The reference plane P_2 (Fig. 1), where the DUT input reflection coefficients are measured, is determined by calibrating the ANA when measuring the DUT *S*-parameters using the TRL technique [7]. This is done with the tuner's stubs locked in a fixed position. Using this approach, we can measure at plane P_2 , N DUT reflection coefficients ($\Gamma_{i2}, i = 1 \dots N$), by changing N times the DUT biasing conditions. If the DUT is repeatable, one can associate a reflection coefficient Γ_{i2} to each bias point. By this process, we can generate N "on line" usable standards. Therefore, the first stage *S*-parameters (S_{11}, S_{22} and $S_{12}S_{21}$) are determined by solving a linear system of N equations and three unknowns.

B. Repeatability of the DUT Input Reflection Coefficients

Measurements were done on a general purpose *L* to *X* Band GaAs-MESFET (NE76184A). In order to reduce the noise level added by the transistor, the noise and *S*-parameter measurements were done at the bias point $V_{DS} = 3$ V and $I_{DS} = 10$ mA. In these conditions, the transistor is unconditionally stable from 5 to 8 GHz. To complete the test band to an octave, the noise measurements are carried out from 4 to 8 GHz. At 4 GHz, we insured that the selected source reflection coefficient Γ_s was in the stable region (Fig. 2).

MESFET input reflection coefficients (Fig. 3) were generated at the following bias points: $V_{DS} = 0$ V and $V_{GS1} = 0$ V, $V_{GS2} = -1$ V and $V_{GS3} = -2$ V. These bias points were chosen to have a phase dispersion as maximum as possible. The first stage *S*-parameter measurement accuracy, and therefore the validity of the extracted transistor noise-parameters, depends on the DUT input reflection coefficient repeatability. As an example, Fig. 3 shows the variation of these loads in a one-week interval at 4 GHz. Over the frequency band and for every bias point, the amplitude and phase drift are lower than 0.4 dB and 6 degrees, respectively. In order to limit this phenomenon, all the necessary measurements, at a given frequency, were made the same day.

III. STAGES AVAILABLE GAIN MEASUREMENTS

A. First Stage Noise Contribution

The first stage *S*-parameters (Fig. 2) are measured at each new position of the tuner's stubs, using the following simple method. In a straightforward manner, the P_1 plane is fixed (Fig. 1) where three reflection coefficient, Γ_{i1} , corresponding to the three DUT known

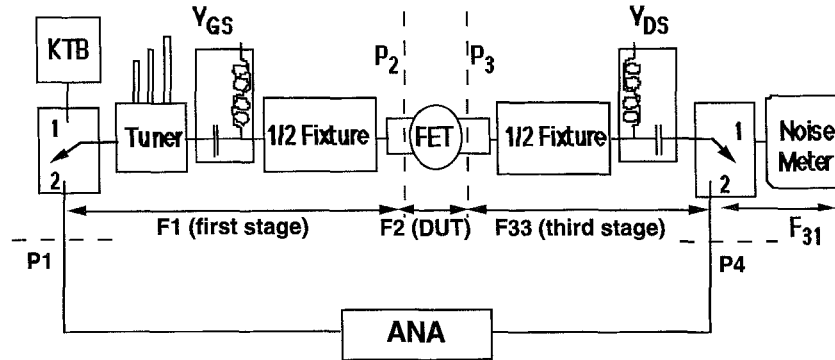


Fig. 1. Two-port microwave noise measurement setup.

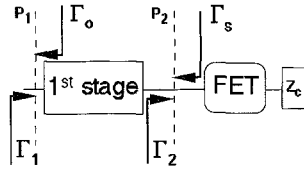


Fig. 2. First stage S -parameter measurement approach.

input reflection coefficients, are measured. Equation (1) gives the relation between such reflection coefficients

$$\begin{aligned} \Gamma_{i1} &= S_{11} + \frac{S_{12}S_{21}\Gamma_{i2}}{1 - S_{22}\Gamma_{i2}} \\ \Rightarrow \Gamma_{i1} &= S_{11} + S_{22}\Gamma_{i1}\Gamma_{i2} + (S_{12}S_{21} - S_{22}S_{11})\Gamma_{i2}. \end{aligned} \quad (1)$$

Where Γ_{i2} is a known bias-dependent reflection coefficient of the FET, Γ_{i1} is a measured one and S_{ij} are the first stage scattering parameters. Using this equation, a set of three linear equations and three unknowns can be formed. The solving of this set gives us the first stage S -parameters S_{11} , S_{22} and $S_{12}S_{21}$. Given these parameters and the noise source reflection coefficient, Γ_0 , the available gain of the first stage, G_1 , and the DUT source reflection coefficient, Γ_s , are determined as follows:

$$\Gamma_s = S_{22} + \frac{S_{12}S_{21}\Gamma_0}{1 - S_{11}\Gamma_0} \quad (2.1)$$

$$G_1 = \frac{1 - |\Gamma_0|^2}{1 - S_{11}\Gamma_0} |S_{21}|^2 \frac{1}{1 - |\Gamma_s|^2}. \quad (2.2)$$

In (2.2), $|S_{21}|^2$ has to be known, but only $S_{11}S_{12}$ is computed. Therefore, we supposed implicitly that $|S_{21}|^2 = |S_{21}S_{12}|$. This implies that the first stage must be entirely composed of reciprocal elements.

B. Third Stage Noise Contribution

In the proposed approach, the measurement carried on the whole system starts with the third stage noise characterization. This is accomplished by the third stage S -parameter measurement using the generalized TRL technique [8]. In a first step, the ANA is calibrated in the reference planes P_1 and P_4 . In a second step, the calibration is done in reference planes P_2 and P_3 . It is well known that the TRL technique allows to determine the S -parameters of input and output error boxes, which represent the set of ANA systematic errors. Therefore, the third stage S -parameters (S_{11} , S_{22} , and $S_{12}S_{21}$) are equal to those of the ANA output error box (Fig. 1).

In order to compute the third stage available gain, G_{33} , we assume $|S_{21}|^2 = |S_{21}S_{12}|$. This means that the third stage must also be entirely constituted by reciprocal elements. The third stage source

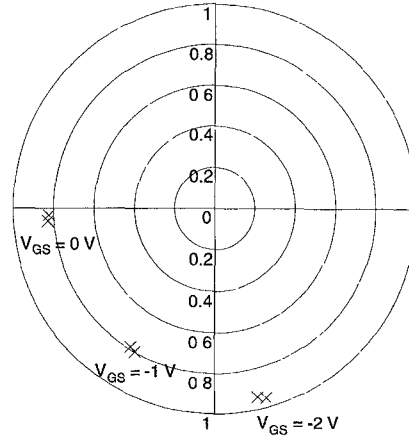


Fig. 3. Transistor input reflection coefficient at 4 GHz for different bias points.

reflection coefficient is directly obtained using the noise source reflection coefficient, Γ_0 , and the S -parameters of the first stage and the DUT.

IV. TRANSISTOR NOISE MEASUREMENT

The noise-receiver measures the noise-figure of the whole system, F_t , including its own noise-figure, F_{31} (Fig. 1). As shown by (3), the total noise-figure, F_t , is function of the different available gains and the noise-figures

$$F_t = F_1 + \frac{F_2 - 1}{G_1} + \frac{F_{33} - 1}{G_1 G_2} + \frac{F_{31} - 1}{G_1 G_2 G_{33}}. \quad (3)$$

For the first and third stages, their noise-figure values vary as the inverses of their available gains. Using this in (3), the FET noise-figure, F_2 , is

$$F_2 = F_t G_1 - \frac{F_{31} - G_{33}}{G_2 G_{33}}. \quad (4)$$

As shown in (4), the DUT noise-figure, F_2 , is computed using the S -parameters and the noise-receiver measurements.

Every DUT noise-figure measurement, F_2 , corresponds to a specific DUT source reflection coefficient, Γ_s (2.1). The relation between them is described by the following well-known nonlinear equation:

$$F_2 = F_{\min} + \frac{4r_n}{|1 + \Gamma_{\text{opt}}|^2} \frac{|\Gamma_s - \Gamma_{\text{opt}}|^2}{1 + |\Gamma_s|^2}. \quad (5)$$

This equation describes the surface of a quasi-elliptic paraboloid. Every measurement (F_{i2}, G_{is}) has to be located on this surface. Thus, it is necessary to identify the four noise-parameters that bring

TABLE I
MEASURED NOISE PARAMETERS AT DIFFERENT FREQUENCIES

Frequency	F_{\min}	r_n	$ \Gamma_{\text{opt}} $	$\Phi(\Gamma_{\text{opt}})$
4 GHz	1.18	0.49	0.69	84.0 °
5 GHz	1.29	0.29	0.68	96.0 °
6 GHz	1.27	0.23	0.50	137.0 °
7 GHz	1.33	0.41	0.44	169.0 °
8 GHz	1.40	0.31	0.43	183.0 °
Standard deviation	$\Delta F_{\min} = 0.06$	$\Delta r_n = 0.15$	$\Delta \Gamma_{\text{opt}} = 0.11$	$\Delta \Phi(\Gamma_{\text{opt}}) = 8$ °

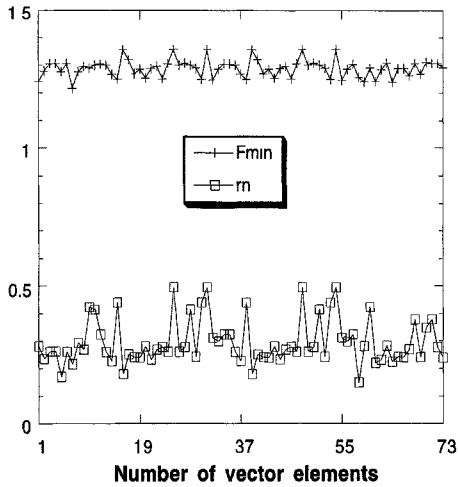


Fig. 4. Extracted F_{\min} and r_n at 5 GHz.

the measurements closer to this surface. The method used in the noise-parameter extraction [9], was already used in other cases with satisfactory results [5], [9].

In theory, every extracted parameter should be a constant, but we note (Fig. 4) that every parameter oscillates around a mean value. The data is therefore contaminated by numerical noise, and must be averaged. The averaged value constitutes the estimation of the parameter. Using this value, we calculate the standard deviation, which gives the confidence we have in the estimation. The results for every noise-parameter is presented in Table I. The shown standard deviation is the largest value obtained for the five frequencies.

The results obtained were compared with those given by the transistor manufacturer. In the test frequency-band, the manufacturer measurements are given at 4, 6, and 8 GHz [10], [11]. In order to complete the data, interpolation were made for the intermediate frequencies, 5 and 7 GHz, using the "splines" method.

Such comparison is shown in Figs. 5 and 6 for the four noise-parameters. Good agreement is obtained between the measurement results and the manufacturer data, except for two points of r_n and G_{opt} angle. Better agreement could be obtained if the measurements are done in a shielded room, and more filtering of the power supply is applied.

V. CONCLUSION

A novel systematic approach for the noise-figure and S -parameter measurements of two-port devices was presented. Such approach has the principal advantage of using an uncalibrated mechanical tuner. This comes from the use of the DUT as a variable microwave load. In the same time, the components used in the measurement bench do not

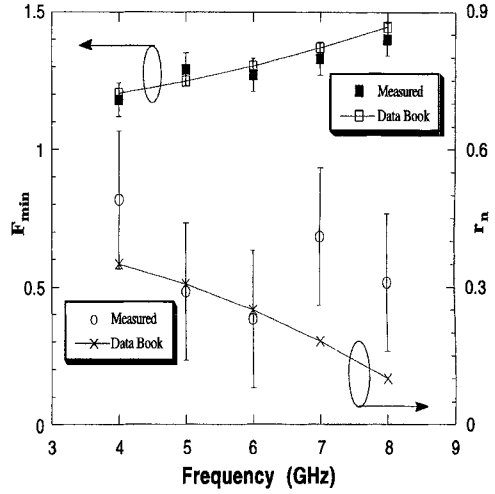


Fig. 5. Comparison between measured and data book values of F_{\min} and r_n .

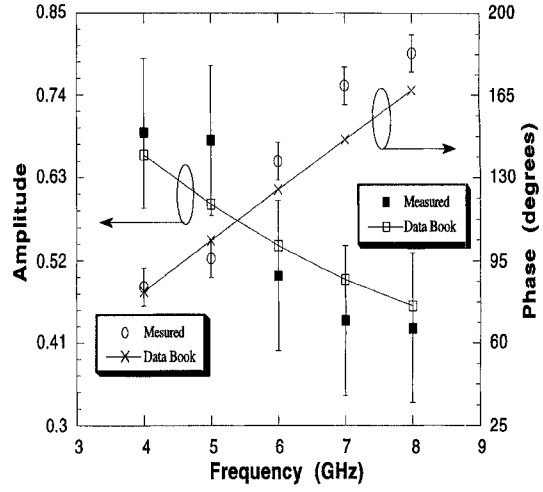


Fig. 6. Comparison between measured and data book values of amplitude and phase of Γ_{opt} .

have to have specific characteristics, which reduce the equipment cost. The approach was validated by characterizing a GaAs MESFET. Our results are in acceptable agreement with those given by the transistor manufacturer.

ACKNOWLEDGMENT

The authors wish to express their thanks to Prof. F. M. Ghannouchi for providing the tested transistors, and Dr. R. Hajji and Dr. A. B. Kouki for their helpful discussions.

REFERENCES

- [1] M. W. Pospieszalski, "Modeling of noise parameters of MESFET's and their frequency and temperature dependence," *IEEE Trans. Microwave Theory Tech.*, vol. 37, no. 9, Sept. 1989, pp. 1340-1350.
- [2] P. J. Tasker, W. Reinert, B. Hughes, J. Braunstein, and M. Schlechtweg, "Transistor noise parameter extraction using 50 ohm measurement system," in 1993 *MTT-S Int. Microwave Symp. Dig.*, pp. 1251-1254.
- [3] G. Martines and M. Sannino, "A method for measurement of losses in the noise-matching microwave network while measuring transistor noise parameters," *IEEE Trans. Microwave Theory Tech.*, vol. MTT-35, no. 1, pp. 71-75, Jan. 1987.
- [4] A. Davidson, B. Leake, and E. Strid, "Accuracy factors in microwave noise parameter measurements," in 1989 *MTT-S Int. Microwave Symp. Dig.*, pp. 827-830.
- [5] L. Escotte, R. Plana, and J. Graffeuil, "Evaluation of Noise Parameter Extraction Methods," *IEEE Trans. Microwave Theory Tech.*, vol. 41, no. 3, Mar. 1993.
- [6] E. Strid, "Noise measurements for low-noise GaAs FET amplifiers," *Measurements Techniques*, pp. 62-70, Nov. 1981.
- [7] G. F. Engen and C. A. Hoer, "Thru-reflect-line: An improved technique for calibrating the dual six-port automatic network analyzer," *IEEE Trans. Microwave Theory Tech.*, vol. 27, no. 12, pp. 987-993, Dec. 1979.
- [8] R. Pantoja *et al.*, "Improved calibration and measurement of the scattering parameters of microwave integrated circuits," *IEEE Trans. Microwave Theory Tech.*, vol. 37, no. 11, pp. 1675-1680, Nov. 1989.
- [9] G. Vasilescu, G. Alquie, and M. Krim, "Exact computation of two-port noise parameters," *Electron. Lett.*, vol. 25, no. 4, Feb. 16, 1989.
- [10] NEC Data Book, "RF and Microwave Semiconductors," Ca. Eastern Lab., pp. 1-94, 1994.
- [11] NEC Microwave Semiconductor Devices, "Design Parameter Library, Vers. 6," Ca. Eastern Lab.

The Analysis of General Two-Dimensional PEC Structures Using a Modified CPFDTD Algorithm

Chris J. Railton, Ian J. Craddock, and John B. Schneider

Abstract—The use of the contour path finite difference time domain (CPFDTD) method with locally distorted contours has been shown to give accurate results for curved metal structures. However, the numerical stability of this scheme is not guaranteed and significant skill is required in order to generate an appropriate grid. In this contribution, we present a modification to the CPFDTD scheme which ensures stability and give a step-by-step procedure for simple generation of the distorted grid. Examples are presented to demonstrate that the modified scheme yields results superior to those obtained using the standard staircased finite difference time domain (FDTD) approach. Example geometries are cylindrical cavities having complex cross-sections with smooth surfaces and right-angle bends. The accuracy of the method is demonstrated by comparison to analytical results where available.

I. INTRODUCTION

The electromagnetic analysis of complex, curved metal structures using the finite difference time domain (FDTD) technique has proved a difficult challenge and one which has not yet been satisfactorily

Manuscript received August 22, 1995; revised June 14, 1996.

C. J. Railton and I. J. Craddock are with the Centre for Communications Research, Faculty of Engineering, University of Bristol, Bristol, BS8 1TR, UK.

J. B. Schneider is with the School of Electrical Engineering and Computer Science, Washington State University, Pullman, WA 99164-2752 USA.

Publisher Item Identifier S 0018-9480(96)06910-4.

resolved. Such problems do, however, occur in a wide variety of application areas ranging from propagation in waveguides to scattering from aircraft fuselages. Attempts to overcome the difficulties associated with this type of problem include the use of globally distorted meshes [1]-[3] and the incorporation of static field solutions (SFS) into the standard Cartesian mesh [4], [5]. The former requires approximately three times the computer resources of the standard Cartesian FDTD at the same number of points per wavelength [2], while the latter, in its present state of development, is prone to late-time instability.

A third approach to the problem is to use a locally distorted mesh where the basic Cartesian grid is modified only in the vicinity of the metal boundaries. One such scheme, the contour path finite difference time domain (CPFDTD) scheme, is formulated in terms of the integral form of Maxwell's equations instead of the usual differential form [6], [7]. A major advantage of this approach when compared to other conformal techniques is that the simplicity and efficiency of the Cartesian mesh is retained throughout the majority of the problem space and only those nodes which are adjacent to the curved surface need be given special attention. In addition, the algorithms for absorbing boundaries, near-to-far field transformations and Huygens' sources, which are well developed for the standard FDTD method, can be applied without change.

Despite the fact that this type of algorithm appears to allow the efficient analysis of very complex structures, comparatively little use of the method has been reported. Some researchers have called into question the stability of the original CPFDTD scheme since it employs a noncausal and nonreciprocal "nearest neighbor" approximation [3], [8], [9]. Despite the fact that stability cannot be guaranteed, it appears that, with appropriate grid selection, instabilities may be weak enough so as not to preclude using the original CPFDTD scheme for particular open-domain problems [9]. For lossless resonant structures, however, for which there is no mechanism for dissipating spuriously generated energy, meaningful results are not usually obtainable [9], [10].

In this contribution we present a modified form of the two-dimensional (2-D) CPFDTD algorithm which overcomes these problems without sacrificing accuracy. This modification recasts the "nearest neighbor" approximation, employed in standard CPFDTD, such that reciprocal interaction of nodes is obtained. Examination of the update equations for those E field nodes whose values are borrowed by neighboring cells and for the H field cells which are directly affected by them, shows that the original CPFDTD spatial discretization scheme is likely to produce a system which does not comply with the law of conservation of energy. It can also be shown that grids which allow extended contours to overlap may not conserve energy. Since, in these cases, the instability is inherent in the *spatial* discretization, there will exist no choice of time step which will yield a stable solution. Before it is useful to consider the problem of determining the CFL limit for the modified *difference* scheme, it is necessary to ensure that the underlying *differential* scheme is energy conserving. The modification described in this contribution yields a system whose update equations are identical to those of a passive electrical network consisting only of capacitors and gyrators which must necessarily conserve energy [11].

In this paper the nature of the instabilities which can occur in the standard CPFDTD algorithm is discussed, then, a step-by-step procedure is presented whereby the energy conserving CPFDTD mesh can be generated. Finally the use of the method is demonstrated